Journal of
Materials Chemistry B

Materials for biology and medicine

Accepted Manuscript

This article can be cited before page numbers have been issued, to do this please use: P. Manini, V. Lucci, V. Lino, S. Sartini, F. Rossella, G. Falco, C. Chiappe and M. d'Ischia, *J. Mater. Chem. B*, 2020, DOI: 10.1039/D0TB00623H.

ROYAL SOCIETY OF CHEMISTRY

rsc.li/materials-b

View Article Online
DOI: 10.1039/D0TB00623H

ARTICLE

Synthetic Mycomelanin Thin Films as Emergent Bio-Inspired Interfaces Controlling the Fate of Embryonic Stem Cells

Received 00th January 20xx,
Accepted 00th January 20xx

DOI: 10.1039/x0xx00000x

Paola Manini,*[a] Valeria Lucci,[b] Valeria Lino,[a,c] Stefania Sartini,[d] Francesco Rossella,[e] Geppino Falco,*[b] Cinzia Chiappe,[d] Marco d'Ischia[a]

The fungal pathways of melanin synthesis have so far been little considered as a source of bio-inspiration in the field of functional materials, despite the interesting properties exhibited by Ascomyces melanins from 1,8-dihydroxynaphthalene (1,8-DHN), including the ability to shield organisms from ionizing radiation. Herein is reported for the first time the processing technique and the characterization of mycomelanin thin films obtained from the solid state polymerization of 1,8-DHN. Overall the results pointed out the role of synthetic mycomelanin thin films as the prototype of next generation bioinspired interfaces featuring high structural regularity and ultrasmooth morphology, high robustness against peroxidative bleaching and adhesion underwater conditions, a good biocompatibility and unprecedented effects in inducing the spontaneous differentiation of embryonic stem cells prevalently toward the endoderm lineage in the absence of added factors. These data open new perspectives toward the applications of this biomaterials in the fields of tissue engineering and regenerative medicine.

Introduction

The design and implementation of functional biointerfaces for stem cells manipulation is currently an active issue in tissue engineering and regenerative medicine.[1] Despite extensive investigations over the past decade, advances in the field are hindered by the currently incomplete understanding of the complex interactions between stem cells and their microenvironment (niche).[2] Under standard cell culture conditions there is usually a need to rely on additive molecules that orchestrate the regenerative signals and drive the differentiation pathways.[3] Recent lines of evidence, however, concur to highlight, in addition to morphogens regulating cellular differentiation, the importance of a cellular support (the biointerface) to efficiently govern the balance between stem cell self-renewal and differentiation.[4] In order to promote a favorable communication between cells and their microenvironment, including the extracellular matrix (ECM) and neighboring cells and tissues, the biointerface should fulfill a series of requisites of chemical, topographical and mechanical nature.[5,6]

From the chemical viewpoint, biointerfaces are usually coated or covalently functionalized with ECM proteins, peptide motifs or growth factors to overcome issues derived from the failure of common materials to adequately mimic the bioactivity features of the ECM.[7] Sometimes the use of optically active groups is desirable when exploring the effect of surface chirality on cell behaviors. Emerging importance is also attributed to the topographical features of biointerfaces, which may encompass 2D micro/nano-patterns up to complex 3D architectures (i.e. pillars, needles and fibers) and appear to play a central role in directing cell adhesion and cell-to-cell communication.[8,9]

Finally, varying the physical and mechanical properties of the materials may offer insights into the contractile force and mechano-transduction mechanisms of cells, as in the case of micropost arrays used for measuring stem cell-derived cardiomyocyte contractility.[10]

In this context, particular attention is devoted to the design of dynamic biointerfaces that can be used to control cell adhesion, proliferation and release, allowing applications in real-time cell biology, regenerative medicine, and theranostics.[11] To this aim, a series of chemical groups can be used for surface functionalization or as anchor for cell binding ligands that can respond to different types of external stimuli, including temperature, pH, bias and light.[12-15]

Despite the great potential of dynamic biointerfaces, their use is often associated with a series of practical complications. For example, the application of external stimuli may be invasive for living cells or may cause the release of cytotoxic molecules deriving from the linker fragmentation. Therefore, exploitation

[a] Department of Chemical Sciences, University of Napoli Federico II, Complesso Universitario Monte S. Angelo, via Cintia 4, I-80126, Napoli, Italy. E-mail: paola.manini@unina.it
[b] Department of Biology, University of Napoli Federico II, Complesso Universitario Monte S. Angelo, via Cintia 4, I-80126, Napoli, Italy. E-mail: geppino.falco@unina.it
[c] Scuola Normale Superiore, Piazza dei Cavalieri 7, I-56126 Pisa, Italy.
[d] Department of Pharmacy, University of Pisa, via Bonanno Pisano 33, I-56126 Pisa, Italy.
[e] NEST, Scuola Normale Superiore and Istituto Nanoscienze - CNR, Piazza San Silvestro 12, I-56127, Pisa, Italy.

Electronic Supplementary Information (ESI) available: materials and methods, FT-IR spectroscopic imaging and AFM images. See DOI: 10.1039/x0xx00000x

of new biointerfaces that respond to all the requisites of cell biocompatibility and communication is very challenging but highly anticipated.

Recently, eumelanins, the dark brown pigments found in mammalian skin, hair and eyes, have emerged as versatile leads for the fabrication of innovative multifunctional dynamic biointerfaces,[16] combining excellent biocompatibility[17] and unique antioxidant, opto-electronic and electrical properties.[18,19] A fundamental advancement toward a eumelanin-based technology for surface functionalization and biointerface design has derived from the development of the ammonia-induced solid state polymerization (AISSP) protocol allowing the deposition of eumelanin coatings on vary substrates from 5,6-dihydroxyindole (DHI) thin films.[20] Due to the dry, solid state conditions of the protocol, issues relating to eumelanin insolubility, high structural heterogeneity, disordered morphology and limited adhesion can be effectively overcome, allowing the buildup of 2D and 3D architectures that are fully compatible with different cell lines and stem cells.[20,21]

Despite the great potential of melanin-based biointerfaces associated to the softness, bioavailability and biocompatibility of these polymers, several issues and practical limitations still hinder the development of robust and versatile thin films for biomedical applications. One major gap derives from the marked sensitivity of eumelanin coatings to degradation processes under alkaline or oxidative conditions, a consequence of the presence of catechol/*o*-quinone units notoriously susceptible to oxidative ring fission, strongly affecting the performance of the biointerface.

In view of these and other issues, the rational design and synthesis of advanced robust and device-quality melanin-based biopolymers stands to-date as a challenging goal in materials science for the development of nanosized functional systems and biocompatible interfaces.

A promising source of inspiration toward this goal may come from the non-nitrogenous catechol-free allomelanins, whose biocompatibility, antioxidant and metal chelating power are well documented.[22,23] In this context particular attention has been recently paid to allomelanins from *Aspergillus* fungi.[24] These pigments derive biogenetically from 1,8-dihydroxynaphthalene (1,8-DHN) and exhibit almost complete insolubility in all solvents. Like their nitrogenous eumelanin counterparts, fungal allomelanins (hereafter referred to as mycomelanins) display broad band visible light absorption, accounting for their black color, and an unusually intense electron paramagnetic resonance (EPR) signal, accounting for outstanding antioxidant properties.[25,26]

A dihydroxynaphthalene-based mycomelanin mimic has been reported as a coating agent for material-independent surface modification.[27] This melanin was produced by laccase-catalyzed polymerization of 2,7-dihydroxynaphthalene (2,7-DHN) and was deposited onto metals, polymeric materials, ceramics and mineral complexes to form functional surfaces with bactericidal and metal chelation/reduction properties, and high adhesion with proteins.

Very recently, Gianneschi *et al.* reported on the cellular antioxidant activity of artificial allomelanin nanoparticles obtained from the oxidative polymerization of 1,8-DHN.[28] Apart from these studies, the potential of mycomelanins and related allomelanins for film preparation in biomedicine and nanotechnology has remained largely unexplored.

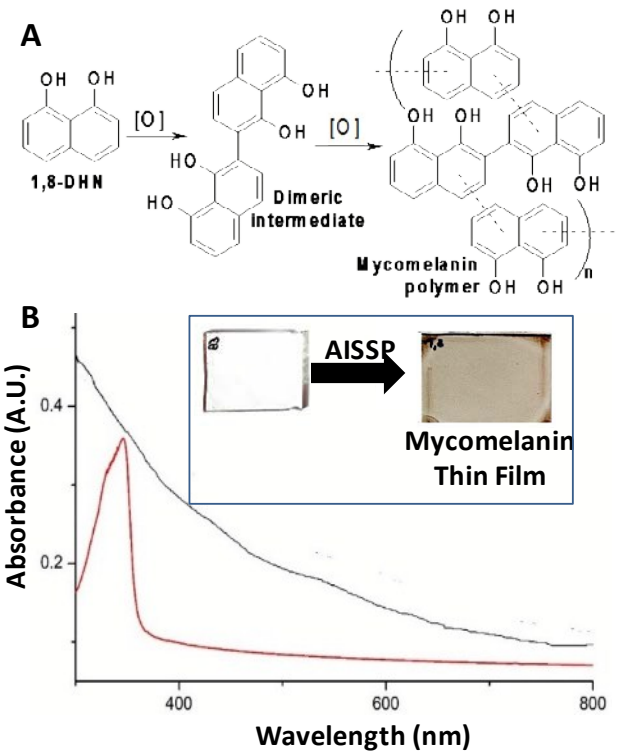

Figure 1. (A) Proposed mechanism for the oxidative polymerization of 1,8-DHN. (B) UV-vis spectra of 1,8-DHN thin films on quartz substrates before (red trace) and after (black trace) AISSP; in the insets the quartz substrates before and after ammonia vapours exposure are shown.

Herein we report the production of unusually smooth, regular and robust mycomelanin thin films by AISSP of 1,8-DHN and disclose the unique property of these films to induce stem cells adhesion, proliferation and differentiation toward an endoderm lineage without added morphogens. This property may be due to the high antioxidant power, resistance to degradation and exceptional smoothness of the allomelanin films and may guide the development of novel device-quality melanin-based biointerfaces for tissue engineering and other biomedical applications.

Results and discussion

Based on the previously developed AISSP protocol,[20] widely used for melanin thin film deposition, thin films of synthetic mycomelanin from 1,8-DHN were deposited on quartz substrates by spin coating of a methanol solution of the precursor followed by exposure to ammonia vapours. UV-visible analysis of the film before and after AISSP confirmed the polymeric melanin-like nature of the material, as apparent

View Article Online
DOI: 10.1039/D0TB00685H

from the intense broadband absorption in both the UV and visible region of the spectrum and from the brown color of the substrate (Figure 1).

The mass spectrum of the film recorded in the MALDI mode confirmed the polymeric nature of the film revealing the presence of regular patterns of peaks separated by 158 Da, corresponding to the "in-chain" dihydroxynaphthalene unit (Figure 2). The dominant peaks were assigned to singly-charged distributions up to 20 units, confirming the lack of any detectable ammonia incorporated into the chemical structure of the polymer. Compared to the MALDI-MS data previously reported for polymers produced by aqueous polymerization, the spectra obtained from the film denoted a minor degree of distribution for each of the clusters, suggesting a more regular structure of the polymer.[29]

The micro ATR spectrum registered on the film showed the presence, among the others, of bands at 1700-1550 cm^{-1}, attributable to C=O and C=C stretching of the conjugated quinonoid structures, and bands between 1400-1200 cm^{-1} suggesting the presence of C-O residues, supporting the structural hypothesis proposed for the allomelanins obtained by the oxidation in solution of 1,8-DHN (Figure 3).

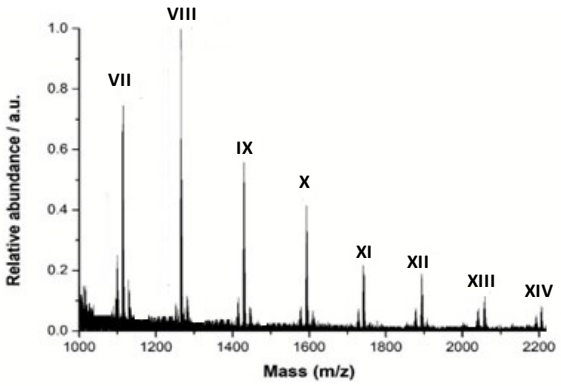

Figure 2. MALDI-mass spectrum of the mycomelanin thin film from 1,8-DHN.

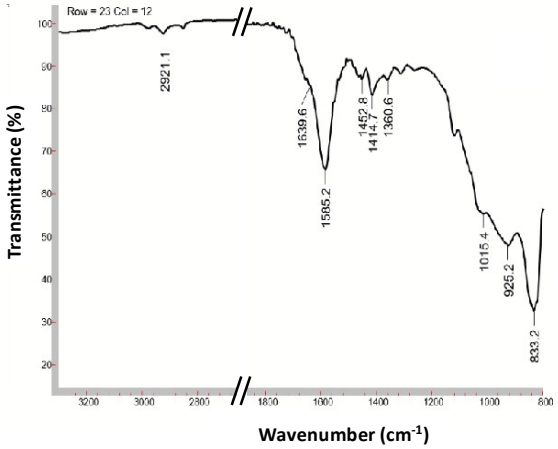

Figure 3. Micro ATR spectrum of the mycomelanin thin film from 1,8-DHN.

The homogeneity of the mycomelanin thin film was checked by FT-IR spectroscopic imaging and atomic force microscopy (AFM).

The point-by-point scansion of the thin film carried out in the FT-IR spectroscopic imaging analysis provided quite similar ATR spectra (see SI section). This data suggested that all the regions investigated corresponded to the same compound with the only differences being in concentration, and that the sample did not contain inclusion compounds or defects, so pointing out the high chemical homogeneity of the film.

Quite interesting results came from the AFM analysis (resumed in Table 1). The films obtained from a nominal concentration of 1,8-DHN of 100 mM were characterized by a thickness of 130 nm and by an ultra-smooth surface.

As shown in Figure 4, the roughness analysis, carried out for the square areas labeled I and II, revealed an unexpectedly low value of 0.25 rms for the mycomelanin film, quite lower than that measured for the substrate (4.00 rms). This evidence confers an added value to the mycomelanin thin films with a view to design dynamic biointerfaces. Noticeably, the ultrasmooth morphology represents an important feature improving the optoelectronic properties of the biointerface. To the best of our knowledge this is the first example of an ultra-smooth thin film obtained by a spin coating deposition.

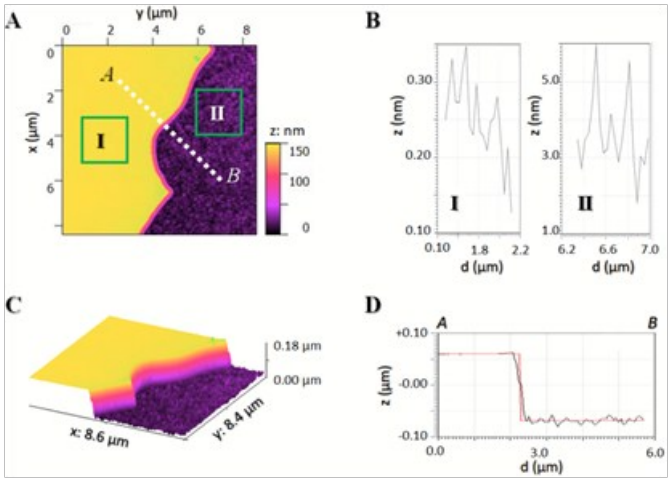

Figure 4. AFM analysis of the mycomelanin thin film from 1,8-DHN. A) Colour plot of one of the AFM maps measured across sharp edges of the film; B) average roughness profile estimated from several scans in two different regions of the map reported in panel A): the region labeled as I lays on the mycomelanin film, while the region labeled as II lays on the substrate. C) three-dimensional rendering of the AFM map reported in panel A). D) cross-sectional profile measured along the segment AB indicated in panel A).

Finally, the stability of the thin films underwater conditions was tested. Preliminarily, water contact angle (WCA) measurements were carried out on the 1,8-DHN mycomelanin thin films providing a value of 33.6° indicative of a good surface wettability (Table 1).

Furthermore, to test the adhesiveness underwater conditions, the mycomelanin-coated quartz substrates were partially immersed in water: after 24 h immersion time no detectable detachment of the film was observed suggesting a high water resistance.

View Article Online
DOI: 10.1039/D0TB00637H

Table 1. Structural parameters for 1,8-DHN mycomelanin thin films.

	Mycomelanin thin film from 1,8-DHN
Thickness (nm)	130
Roughness (rms)	0.25
Water contact angle (°)[a]	33.6 ± 2.1
Water contact angle image	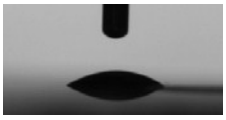

[a]Average and standard deviation of six separate measurements.

Finally, the robustness of the film was assessed by soaking the mycomelanin-coated quartz substrates in an alkaline solution of hydrogen peroxide, a standard bleaching agent for most melanin polymers; the same treatment was performed also on an eumelanin-coated quartz substrates obtained via AISSP of a 5,6-dihydroxyindole (DHI) thin film. As shown in Figure 5, while the DHI-melanin film was gradually detached from the substrate within 10 minutes, no detectable damage for the mycomelanin thin film was visible even after 70 minutes immersion time.

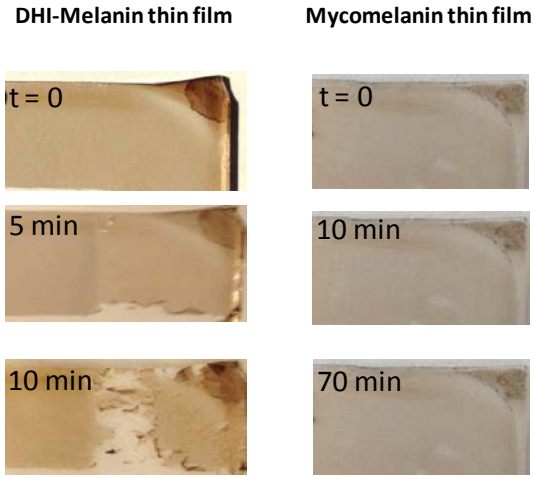

Figure 5. Effects of alkaline hydrogen peroxide solution on DHI-melanin thin film (left) and synthetic mycomelanin thin film (right).

The high robustness of synthetic mycomelanin thin films can be attributed to the structural features of the monomer precursor, 1,8-DHN, for which the formation of catechol/*o*-quinone units, notoriously susceptible to oxidative ring fission, was prevented.

Experiments to assess the biocompatibility of mycomelanin thin films from 1,8-DHN were first carried out on HEK-293 cell line. In detail, HEK-293 cells were trypsinized to obtain a single cell suspension and 2.5 ×10^4 cells/cm^2 were plated on 100 and 200 nm mycomelanin-coated dishes, or on standard tissue culture plates. As shown in Figure 6, HEK-293 cells adhered to both mycomelanin-treated dishes with a similar morphology with respect to control plates. The mycomelanin coatings proved also able to support efficiently the growth of HEK-293 cells, with a proliferation rate at 72 h comparable to standard growth conditions.

Further experiments were carried out to investigate whether mycomelanin thin films from 1,8-DHN could promote also the clonogenic cell growth in an embryonic stem cell (ESC) colony assay. ESCs are of particular interest for their sensitivity to small changes in culture conditions which can affect ESC colony morphology and behaviour. ESCs were cultured for 3 days in regular medium on cell culture plates coated with either 100 and 200 nm mycomelanin films, or gelatin as control.

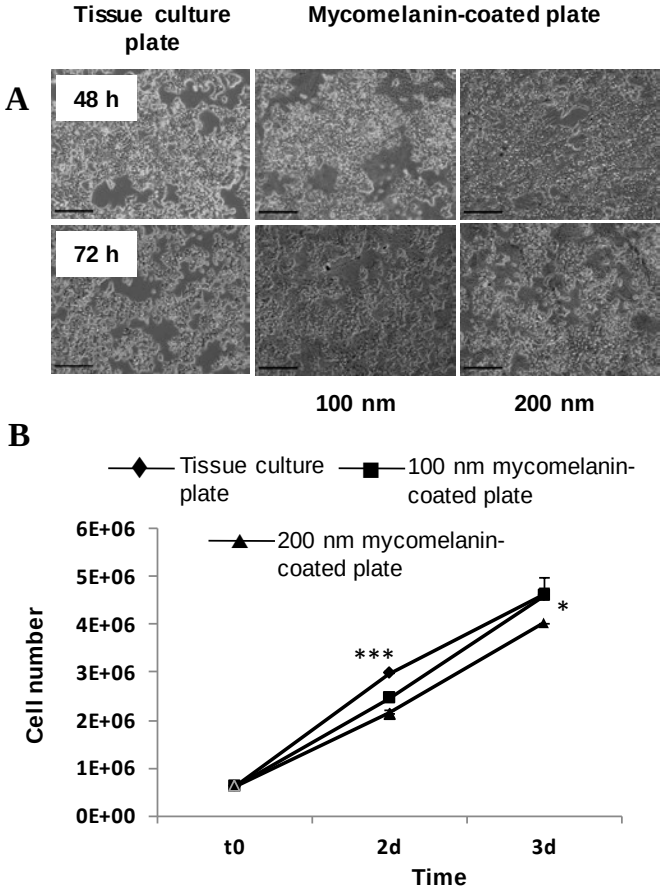

Figure 6. Phase contrast images of HEK-293 cells 48 and 72 h after seeding on dishes coated with a 100 nm and 200 nm mycomelanin thin film or on tissue culture plates, as control. Images were taken with a Leica DMi8 at 10× magnification. Scale bars: 250 µm. B) Growth curves of HEK-293 cells during 72 h are shown. Cells (6 × 10^4) were seeded on tissue culture plate (♦), 100 nm mycomelanin (■) or 200 nm mycomelanin (▲) coated plates and triplicate cultures counted at daily intervals. Data are expressed as the mean ± SD (* $p < 0.05$ and *** $p < 0.001$).

At 24 h, ESCs adhered to plates in all conditions with different degrees of cell attachment. After 48 h, cells proliferated forming regular domed shape colonies, although ESCs cultured on mycomelanin coated plates arise smaller when compared to control condition. Finally, at 72 h, cells on 100 nm mycomelanin coatings retained the morphology and the attachment to the plate in a similar way than control, while the cells on 200 nm mycomelanin coatings seemed to lose adhesion, floating in the medium (Figure 7).

In addition, the expression levels of genes involved in canonical pluripotency such as *Oct3/4*, *Nanog* and *Rex1*, was investigated revealing no significant differences among culture conditions.

With the aim of checking if mycomelanin thin films can be used also to direct cell differentiation into a specific lineage fate (ectoderm, mesoderm or endoderm), ESCs were cultured for five days in a regular medium without Leukemia inhibitory factor (hereafter Lif-), a cytokine required for ESC self-renewal. Statistical analysis was performed on all samples of three independent experiments.

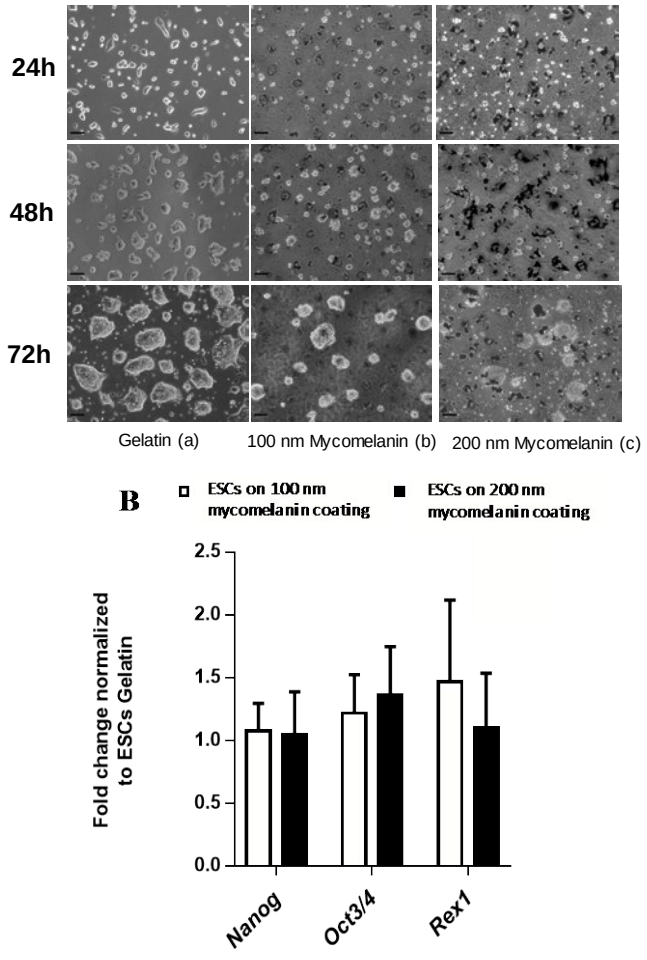

Figure 7. A) Representative light microscope pictures of E14Tg2a.4 mouse ESCs grown on cell culture low adhesion plates coated with gelatin, 100 nm mycomelanin thin film and 200 nm mycomelanin thin film. The images were acquired at 24, 48 and 72 h. Scale bars: 100 µm. B) qRT-PCR analysis of pluripotency-specific markers. The mRNA levels were normalized for *Gapdh* expression and reported as fold change with respect to the value in to ESCs grown in gelatin condition.

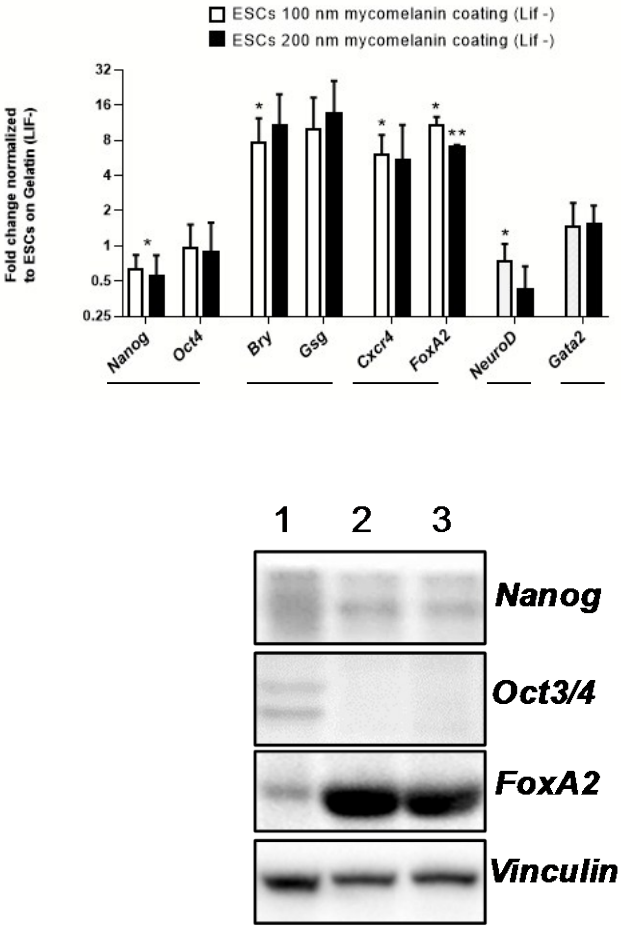

Figure 8. A) ESCs plated on dishes coated with gelatin, 100 nm mycomelanin thin film and 200 nm mycomelanin thin film, were cultured for five days in Lif- differentiating conditions. The mRNA expression levels of pluripotency and differentiation-associated markers were assessed by qRT-PCR and expressed as fold change with respect to the ESCs grown in gelatin conditions. Values shown are mean ± SD, based on triplicate assays. Statistical analyses were performed using Student's t-test, where $p < 0.05$ was considered significant. (* $p < 0.05$, ** $p < 0.01$). B) Total protein extracts prepared from the same growth conditions were separated on SDS-PAGE and subjected to Western blot analysis with specific antibodies. The hybridization with vinculin assessed the protein uniform loading and integrity. Loaded as follow: line 1, ESCs on gelatin coating (Lif-); line 2, ESCs on 100 nm mycomelanin coating (Lif-); line 3, ESCs on 200 nm mycomelanin coating (Lif-); n = 2 independent experiments were performed with similar results.

The expression levels of pluripotency markers (*Nanog* and *Oct3/4*) and lineage-specific markers, such as *Bry* and *Gsg* (early endoderm markers), *Cxcr4* and *FoxA2* (endoderm markers), *Gata2* (mesoderm marker) and *NeuroD* (ectoderm marker), were analyzed by RT-qPCR. In both growing conditions, *Oct3/4* and *Nanog* expressions were

downregulated, pointing out a loss of pluripotency. Interestingly, while there were no differences in the ectoderm and mesoderm markers, *Cxcr4* and *FoxA2* turned out to be overexpressed as well as early endoderm markers (Figure 8A).
The effectiveness of the endoderm induction was further validated by addressing protein expression of pluripotency and endoderm markers. In agreement with qRT-PCR results, it was observed that the expression level of *Nanog* and *Oct3/4* decreased more in mycomelanin than in gelatin condition.
Similar to the upregulation of *FoxA2* mRNA expression (Figure 8A), *FoxA2* protein expression was also increased in both culture conditions as indicated by Western blot signals (Figure 8B). These observations suggested that the mycomelanin coating could commit the differentiation prevalently toward the endoderm lineage.

Experimental

Ammonia induced solid state polymerization (AISSP): general procedure

Suitable amounts of 1,8-DHN were dissolved in methanol and the solutions were filtered with 0.45 µm syringe filters before use. For each deposition 100 µL of the methanol solution of 1,8-DHN was pipetted on the upper side of the substrate just before spinning. The spin coating programme was the following: α = 500 rpm/s, ω = 2000 rpm, t = 30 s. The 1,8-DHN coated substrate was placed in a glass chamber under an ammonia atmosphere equilibrated with air. After 24 h the polymerization was complete, and the substrate was removed from the chamber. Mycomelanin thin films with different thickness were prepared by spin coating 1,8-DHN methanolic solutions with the proper concentration (see ESI section).

RNA extraction, cDNA preparation and Quantitative Real Time PCR (RT–qPCR)

Total RNA was extracted using TRIzol reagent (Invitrogen) and treated with RNase-free DNase I (Applied Biosystem). For qRT-PCR the cDNAs were synthesized using the iScriptcDNA Synthesis kit (BIORAD, Hercules, CA). 1µg of total RNA was used for each cDNA synthesis. Primer 3 software (http://primer3.ut.ee/)was used to design the oligo primers setting the annealing temperature to 59–61 °C for all primer pairs. Oligo sequences are reported in Table S1. Real time-PCR analysis was performed using the iTaq™ Universal SYBR® Green Supermix (BIORAD) in a7500 Real-Time PCR System (Applied Biosystems) under the following conditions: 2 min at 50 °C, 10 min at 95 °C, followed by 40 cycles of 15 s at 95 °C and 1 min at 60 °C. The *Gapdh* probe served as a control to normalize the data. The gene expression experiments were performed in triplicate on three independent experiments and a melting analysis was performed at the end of the PCR run. To calculate the relative expression levels we used the 2^{-DDCT} method.[30]

Cell culture

E14Tg2a.4 ES cells, derived from strain 129P2/OlaHsd were purchased from ATCC company and were cultured for two passages on gelatin-coated feeder-free plates and subsequently maintained in gelatin-coated plates in Glasgow Minimum Essential Medium (Gibco) supplemented with 15% FBS (EuroClone), 1,000 units/mL ESGRO leukaemia inhibitory factor (LIF) (Merck Millipore), 1.0 mM sodium pyruvate (Invitrogen), 0.1 mM non-essential amino acids (Invitrogen), 2.0 mM L-glutamine (Invitrogen), 0.1 mM β-mercaptoethanol (Sigma Aldrich) and 500 U/mL penicillin/streptomycin (Invitrogen). ESCs were incubated at 37°C in 5% CO_2; medium was changed daily and cells were split every 2 to 3 days routinely. The human embryonic kidney (HEK-293) cell line were obtained from the CEINGE Cell Culture Facility (Naples, Italy) and were grown in DMEM medium containing 15% fetal bovine serum (Euroclone).For the growth curve, 6×10^5 cells were seeded in triplicate on 60-mm dishes coated or not with melanin and cell count was performed after 48 h and 72 h from plating.

Protein extracts and immunoblotting

Cells were washed twice with ice-cold phosphate-buffered saline (PBS) and lysed in JS buffer containing 50 mM Hepes pH 7.5, 150 mM NaCl, 5 mM EGTA pH 7.8, 10% glycerol, 1% Triton, 1.5 mM $MgCl_2$, 1 mM dithiothreitol (DTT), 1 mM phenylmethylsulfonyl fluoride (PMSF). Protein concentration was determined using the Bio-Rad protein assay (Bio-Rad Laboratories, Inc., Hercules, CA). For Western blot analysis, proteins were separated on SDS–PAGE, gels were blotted onto Immobilon P (Millipore, Bredford, MA, USA) for 2 h and the membranes were blocked in 5% non fat dry milk in Tris–buffered saline for 2 h or overnight before the addition of the antibody for 1 h. The primary antibodies used were: anti-Vinculin (Santa Cruz, CA), anti-Nanog (Abcam), anti-Oct4 (Abcam) and anti-FoxA2 (Cell Signaling Technology). The filters were washed three times in Tris–buffered saline plus 0.05% Tween 20 before the addition of horseradish peroxidase-conjugated secondary antibodies for 45 min. Horseradish peroxidase was detected with ECL (Pierce).

Conclusions

An ultrasmooth and unusually robust biointerface with potent effects on stem cell adhesion and differentiation is disclosed herein, which is produced by AISSP of the fungal allomelanin precursor 1,8-DHN. Key features of the synthetic mycomelanin thin films include high structural regularity as determined by MALDI-MS, exceptionally low roughness on AFM analysis, high film homogeneity denoted by FT-IR spectroscopic imaging, good wettability and strong adhesion underwater conditions, exceptional resistance even to alkaline hydrogen peroxide, a standard bleaching agent for most melanin polymers. Remarkably, the mycomelanin films proved capable of inducing embryonic stem cell adhesion and spontaneous differentiation prevalently toward the endoderm lineage in the absence of added factors, opening novel vistas in the fields of tissue engineering and regenerative medicine.

Conflicts of interest

The authors declare that there are no conflicts.

View Article Online
DOI: 10.1039/D0TB00623H

Acknowledgements

This work was supported in part by Italian MIUR grants PRIN 2017YJMPZN to MdI and 2017CBHCWF_003 to PM.

Notes and references

1 M. Suchea, I. Tudose, S. Bucur, V. Dinca and L. Rusen, *Functional Nanostructured Interfaces for Environmental and Biomedical Applications Micro and Nano Technologies*, 2019, 1.
2 F. M. Watt and B. L. Hogan, *Science,* 2000, **287**, 1427.
3 P.-Y. Wang, H. Thissen and P. Kingshott, *Acta Biomaterialia,*2016, **45**, 31.
4 J. Robertus, W. R. Browne and B. L. Feringa, *Chem. Soc. Rev.*, 2010, **39**, 354.
5 C. S. Chen, M. Mrksich, S. Huang, G. M. Whitesides and D. E. Ingber, *Science*, 1997,**276**, 1425.
6 M. M. Stevens and J. H. George, *Science*, 2005, **310**, 1135.
7 T. Bhuvanesh, R. Machatschek, L. Lysyakova, K. Kratz, B. Schulz, N. Ma and A. Lendlein, *Biomed. Mater.*, 2019, **14**, 024101.
8 X. Liuab and S. Wang, *Chem. Soc. Rev.*, 2014, **43**, 2385.
9 C. J. Bettinger, R. Langer and J. T. Borenstein, *Angew. Chem. Int. Ed.*, 2009,**48**, 5406.
10 K. M. Beussman, M. L. Rodriguez, A. Leonard, N. Taparia, C. R. Thompson and N. J. Sniadecki, *Methods*, 2016, **94**, 43.
11 J. N. Roberts, J. Kishore Sahoo, L. E. McNamara, K. V. Burgess, J. Yang, E. V. Alakpa, H. J. Anderson, J. Hay, L.-A. Turner, S. J. Yarwood, M. Zelzer, R. O. C. Oreffo, R. V. Ulijn and M. J. Dalby, *ACS Nano*, 2016, **10**, 6667.
12 T. T. Lee, J. R. Garcia, J. I. Paez, A. Singh, E. A. Phelps, S. Weis, Z. Shafiq, A. Shekaran, A. Del Campo and A. J. Garcia, *Nat. Mater.*, 2015, **14**, 352.
13 D. Liu, Y. Xie, H. Shao and X. Jiang, *Angew. Chem. Int. Ed.*, 2009, **48**, 4406.
14 P. M. Mendes, *Chem. Soc. Rev.*, 2013, **42**, 9207.
15 M. Zelzer, S. J. Todd, A. R. Hirst, T. O. Mcdonald and R. V. Ulijn, *Biomater. Sci.*, 2013, **1**, 11.
16 M. d'Ischia, A. Napolitano, A. Pezzella, P. Meredith and M. J Buehler, *Angew. Chem. Int. Ed.,* 2019, 10.1002/anie.201914276.
17 C. J. Bettinger, J. P. Bruggeman, A. Misra, J. T. Borenstein and R. Langer, *Biomaterials*, 2009, **30**, 3050.
18 M. d'Ischia, A. Napolitano, A. Pezzella, P. Meredith and T. Sarna, *Angew. Chemie Int. Ed.*, 2009, **48**, 3914.
19 S. R. Cicco, M. Ambrico, P. F. Ambrico, M. Mastropasqua Talamo, A. Cardone, T. Ligonzo, R. Di Mundo, C. Giannini, T. Sibillano, G. M. Farinola, P. Manini, A. Napolitano, V. Criscuolo and M. d'Ischia *J. Mater. Chem. C*, 2015, **3**, 2810.
20 A. Pezzella, M. Barra, A. Musto, A. Navarra, M. Alfè, P. Manini, S. Parisi, A. Cassinese, V. Criscuolo and M. d'Ischia, *Mater. Horiz.*, 2015, **2**, 212.
21 I. Fasolino, I. Bonadies, L. Ambrosio, M. G. Raucci, C. Carfagna, F. M. Caso, F. Cimino and A. Pezzella, *ACS Appl. Mater. Interfaces*, 2017, **9**, 40070.
22 L. Panzella, G. D'Errico, G. Vitiello, M. Perfetti, M. L. Alfieri, A. Napolitano and M. d'Ischia, *Chem. Commun.*, 2018, **54**, 9426.
23 P. Manini, L. Panzella, T. Eidenberger, A. Giarra, P. Cerruti, M. Trifuoggi and A. Napolitano, *J. Agric. Food Chem.*, 2016, **64**, 890.
24 J. D. Nosanchuk, R. E. Stark and A. Casadevall, *Frontiers Microbiol.* 2015, **6**, 1463.
25 P. Manini, M. Bietti, M. Galeotti, M. Salamone, O. Lanzalunga, M. M. Cecchini, S. Reale, O. Crescenzi, A. Napolitano, F. De Angelis, V. Barone and M. d'Ischia, *ACS Omega*, 2018, **3**, 3918.
26 P. Manini, V. Lino, P. Franchi, G. Gentile, T. Sibillano, C. Giannini, E. Picardi, A. Napolitano, L. Valgimigli, C. Chiappe and M. d'Ischia, *ChemPlusChem,* 2019, **84**, 1331.
27 J.-R. Jeon, T. T. Le and Y.-S. Chang, *Microbial Biotech.*, 2016,**9**, 305.
28 X. Zhou, N. C. McCallum, Z. Hu, W. Cao, K. Gnanasekaran, Y. Feng, J. F. Stoddart, Z. Wang, N. C. Gianneschi, *ACS Nano*, 2019, **13**, 10980.
29 M. M. Cecchini, S. Reale, P. Manini, M. d'Ischia and F. De Angelis, *Chem. Eur. J.*, 2017, **23**, 8092.
30 K. J. Livak and T. D. Schmittgen, *Methods* 2001, **25**, 402.

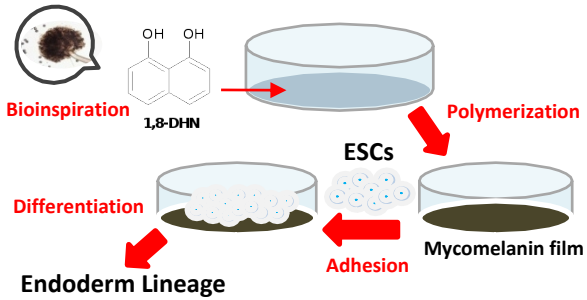

Mycomelanin thin films from 1,8-dihydroxynaphthalene can serve as biointerface inducing ESCs adhesion, proliferation and promoting differentiation toward the endoderm lineage.